AMERICAN SOCIETY FOR MICROBIOLOGY | Infection and Immunity®

HOST RESPONSE AND INFLAMMATION

Yersinia pseudotuberculosis Exploits CD209 Receptors for Promoting Host Dissemination and Infection

Ying-Xia He,[a] Cheng-Lin Ye,[a] Pei Zhang,[a] Qiao Li,[a] Chae Gyu Park,[b] Kun Yang,[c] Ling-Yu Jiang,[a] Yin Lv,[a] Xiao-Ling Ying,[a] Hong-Hui Ding,[a] Hong-Ping Huang,[a] John Mambwe Tembo,[a,d] An-Yi Li,[a] Bing Cheng,[a] Shu-Sheng Zhang,[e] Guo-Xing Zheng,[e] Shi-Yun Chen,[f] Wei Li,[g] Lian-Xu Xia,[g] Biao Kan,[g] Xin Wang,[g] Huai-Qi Jing,[g] Rui-Fu Yang,[h] Hua Peng,[i] Yang-Xin Fu,[j] John D. Klena,[k] Mikael Skurnik,[l] Tie Chen[a]

[a]Department of Clinical Immunology, Tongji Hospital, Tongji Medical College, Huazhong University of Sciences and Technology, Wuhan, Hubei, China
[b]Laboratory of Immunology, Brain Korea 21 PLUS Project for Medical Science, Severance Biomedical Science Institute, Yonsei University College of Medicine, Seoul, Republic of Korea
[c]Department of Pathogen Biology and Immunology, Shihezi University School of Medicine, Shihezi, Xinjiang, China
[d]Department of Paediatrics & Child Health, The University of Zambia–University College London Medical School at Zambia, Lusaka, Zambia
[e]Department of Biomedical Science, College of Medicine-Rockford, University of Illinois at Chicago, Rockford, Illinois, USA
[f]Key Laboratory of Special Pathogens and Biosafety, Wuhan Institute of Virology, Chinese Academy of Sciences, Wuhan, China
[g]Department of Diarrheal Diseases, National Institute for Communicable Diseases Control and Prevention, Beijing, China
[h]State Key Laboratory of Pathogen and Biosecurity, Beijing Institute of Microbiology and Epidemiology, Beijing, China
[i]Key Laboratory of Infection and Immunity, Institute of Biophysics, Chinese Academy of Sciences, Beijing, China
[j]Department of Pathology, University of Texas Southwestern Medical Center, Dallas, Texas, USA
[k]Centers for Disease Control and Prevention, Atlanta, Georgia, USA
[l]Department of Bacteriology and Immunology, University of Helsinki, Helsinki, Finland

ABSTRACT *Yersinia pseudotuberculosis* is a Gram-negative enteropathogen and causes gastrointestinal infections. It disseminates from gut to mesenteric lymph nodes (MLNs), spleen, and liver of infected humans and animals. Although the molecular mechanisms for dissemination and infection are unclear, many Gram-negative enteropathogens presumably invade the small intestine via Peyer's patches to initiate dissemination. In this study, we demonstrate that *Y. pseudotuberculosis* utilizes its lipopolysaccharide (LPS) core to interact with CD209 receptors, leading to invasion of human dendritic cells (DCs) and murine macrophages. These *Y. pseudotuberculosis*-CD209 interactions result in bacterial dissemination to MLNs, spleens, and livers of both wild-type and Peyer's patch-deficient mice. The blocking of the *Y. pseudotuberculosis*-CD209 interactions by expression of O-antigen and with oligosaccharides reduces infectivity. Based on the well-documented studies in which HIV-CD209 interaction leads to viral dissemination, we therefore propose an infection route for *Y. pseudotuberculosis* where this pathogen, after penetrating the intestinal mucosal membrane, hijacks the *Y. pseudotuberculosis*-CD209 interaction antigen-presenting cells to reach their target destinations, MLNs, spleens, and livers.

KEYWORDS *Yersinia pseudotuberculosis*, dendritic cells, DCs, DC-SIGN, CD209a, SIGN-R1, CD209b, lipopolysaccharide core, LPS core, dissemination

Yersinia pseudotuberculosis is a Gram-negative enteropathogen that usually causes food-borne gastrointestinal infections in humans and animals. It belongs to the genus *Yersinia*, which includes 17 different species (1), of which *Y. enterocolitica* and *Y. pestis* cause gastroenteritis and plague, respectively (2–5), and *Y. ruckeri* causes enteric red mouth disease of salmonid fish (6). *Y. pestis* has evolved from *Y. pseudotuberculosis* within the last 10,000 to 20,000 years (7–9). The ability to disseminate to and infect the regional lymph nodes is a characteristic hallmark of *Y. pseudotuberculosis* infection (10).

Citation He Y-X, Ye C-L, Zhang P, Li Q, Park CG, Yang K, Jiang L-Y, Lv Y, Ying X-L, Ding H-H, Huang H-P, Mambwe Tembo J, Li A-Y, Cheng B, Zhang S-S, Zheng G-X, Chen S-Y, Li W, Xia L-X, Kan B, Wang X, Jing H-Q, Yang R-F, Peng H, Fu Y-X, Klena JD, Skurnik M, Chen T. 2019. *Yersinia pseudotuberculosis* exploits CD209 receptors for promoting host dissemination and infection. Infect Immun 87:e00654-18. https://doi.org/10.1128/IAI.00654-18.

Editor Manuela Raffatellu, University of California San Diego School of Medicine

Address correspondence to Mikael Skurnik, mikael.skurnik@helsinki.fi, or Tie Chen, chentie@hust.edu.cn.

Y.-X.H. and C.-L.Y. contributed equally to this article.

Received 27 August 2018
Returned for modification 17 September 2018
Accepted 9 October 2018
Accepted manuscript posted online 22 October 2018
Published 19 December 2018

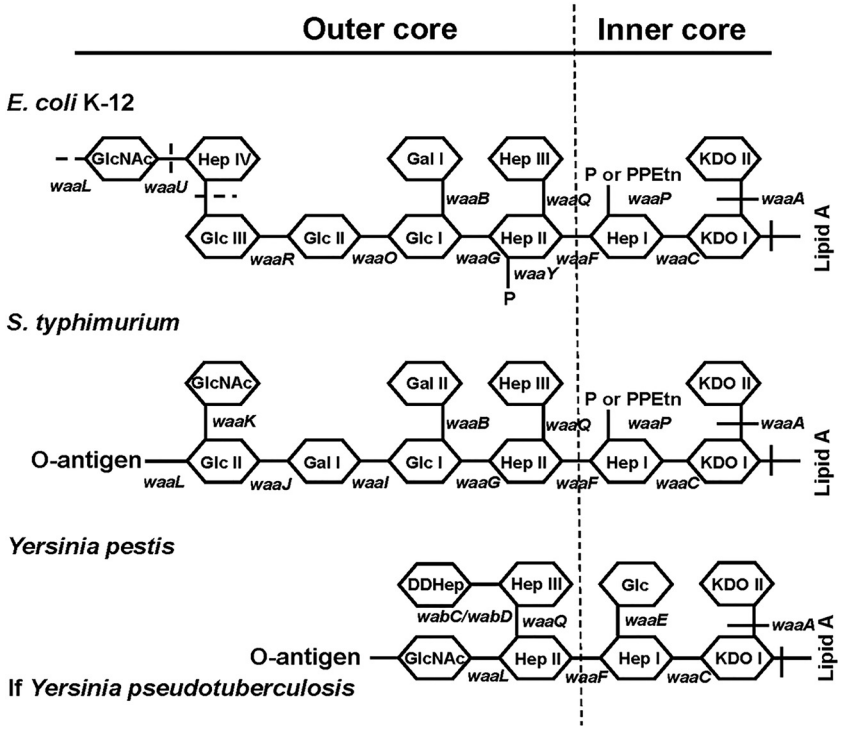

FIG 1 Structures of inner core and outer core regions of the LPS or LOS of *E. coli* K-12, *S. enterica* serovar Typhimurium, *Y. pestis*, and *Y. pseudotuberculosis* and the genes involved in their biosynthesis. Genes involved in the biosynthesis of core LPS are shown at their approximate site of action (solid line). The sites that are variably substituted or still under investigation are indicated by dashed lines. Abbreviations: GlcNAc, *N*-acetylglucosamine; Glc, glucose; Hep, L-glycero-D-manno-heptose; Gal, galactose; P, phosphate; PPEtn, phosphoethanolamine; KDO, 2-keto-3-deoxyoctonate. It should be noted that *E. coli* K-12 and *Y. pestis* naturally do not possess an O-antigen.

Y. pseudotuberculosis disseminates to mesenteric lymph nodes (MLNs) directly from a replicating bacterial pool in the intestinal lumen (11). However, the molecular mechanisms and host cells involved in dissemination of *Y. pseudotuberculosis* to MLNs remain to be determined. On the other hand, the mechanisms used by *Salmonella* for dissemination have been studied, as outlined in an excellent review article (12). *Salmonella* spp. appear to utilize antigen-presenting cells (APCs), such as dendritic cells (DCs), as a carrier to reach the MLNs, after either penetrating the mucosal membranes or passing through the Peyer's patches (12, 13). While the molecular mechanisms of the DC-associated dissemination of *Salmonella* are still unknown, it was shown that the core region of the lipopolysaccharide interacts with the human DC-SIGN (hDC-SIGN; CD209) receptor of DCs (14). DC-SIGN is also a receptor of HIV that hijacks the DCs to promote viral dissemination to target cells, such as CD4 lymphocytes in lymph nodes (15, 16).

Over 70% of the surface of Gram-negative bacteria is occupied by lipopolysaccharide (LPS), which generally consists of three structural regions: (i) lipid A, (ii) the oligosaccharide core, and (iii) the O-polysaccharide (OPS) or O-antigen (O-ag) (Fig. 1). LPS produced by smooth bacteria is known as smooth LPS, while LPS lacking O-ag is known as rough LPS or lipooligosaccharide (LOS). O-ag is a virulence factor of *Y. pseudotuberculosis*; however, its production is suppressed in bacteria grown at 37°C (17–19), suggesting also that the LPS core would be exposed in bacteria growing *in vivo* (Fig. 1). The apparent question, then, is why *Y. pseudotuberculosis* would subdue the production of O-ag, its virulence factor, during infection.

Both *Y. pseudotuberculosis* and *Salmonella* are enteropathogens; therefore, we asked if the LPS core of *Y. pseudotuberculosis* also interacts with DC-SIGN and, if so, whether this interaction would lead to the dissemination of *Y. pseudotuberculosis* to MLNs. *Y. pseudotuberculosis*, after overcoming the first line of host defense, the mucosal mem-

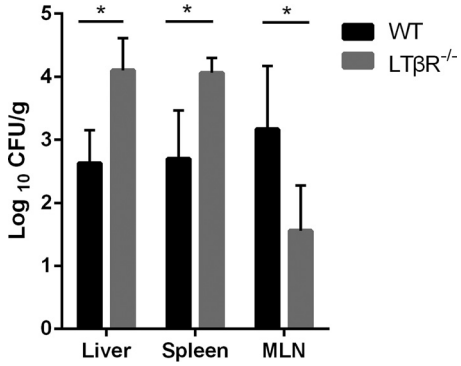

FIG 2 Dissemination of *Y. pseudotuberculosis* in Peyer's patch-deficient mice. Wild-type and lymphotoxin-LTβR-1-deleted mice (25) were orally infected with 10^8 CFU of *Y. pseudotuberculosis* YPIII (37). The dissemination rate (bacterial load) in the spleens, livers, and MLNs was quantified at 72 h after infection. *, $P < 0.05$.

brane of the small intestine, with the help of the virulence factors invasin (20, 21) and Ail (22–24), encounters in the intestinal tissue secondary host defense systems such as DCs and macrophages. Here, we present evidence that rough LPS-producing *Y. pseudotuberculosis* exploits APCs via LOS (rough LPS)-CD209 interaction as a means to disseminate to lymph nodes, spleen, and liver to initiate host infection.

RESULTS

Peyer's patches may not play a major role in dissemination of *Y. pseudotuberculosis*. One of the dissemination mechanisms used by *Salmonella* involves passage through Peyer's patches (12, 13). To examine whether the dissemination of *Y. pseudotuberculosis* involves the Peyer's patches, we used a Peyer's patch-deficient mouse model carrying a deletion of the lymphotoxin-LTβR-1 gene (25). Figure 2 shows that dissemination of the *Y. pseudotuberculosis* strain YPIII bacteria to MLNs, livers, and spleens was not reduced in the Peyer's patch-deficient mice, suggesting that Peyer's patches do not play a major role in dissemination of *Y. pseudotuberculosis*. It should be noted that MLNs are also underdeveloped in the LTβR-1 knockout (KO) mice (25).

hDC-SIGN and murine SIGNR1 (mSIGNR1) are receptors for phagocytosis of *Y. pseudotuberculosis*. If Peyer's patches were not the dissemination route of *Y. pseudotuberculosis*, the pathogen, after passage through the mucosal membrane, encounters the secondary host defense system, including DCs and macrophages. Given that *Y. pseudotuberculosis* produces rough LPS (LOS) when grown at 37°C (17–19), we examined the interactions of APCs with *Y. pseudotuberculosis* bacteria grown at 37°C and at 26°C.

(i) *Y. pseudotuberculosis* bacteria cultured at 37°C but not at 26°C invade human dendritic cells and mouse macrophages. We first examined the ability of *Y. pseudotuberculosis* strain Y1 bacteria grown at 37°C or 26°C to invade human DCs and mouse macrophages. The *Escherichia coli* K-12 strain CS180 (with rough LPS) and CS1861 (CS180 derivative with smooth LPS) bacteria were used as controls (14, 26). The gentamicin protection assay (Fig. 3A and C) and flow cytometry (Fig. 3B and D) experiments showed that Y1 bacteria cultured at 37°C invaded human DCs and macrophages much more effectively than Y1 bacteria cultured at 26°C. The results suggest that lack of O-ag on Y1 bacteria grown at 37°C contributes to the invasion of human DCs and mouse macrophages.

(ii) *Y. pseudotuberculosis* Y1 cultured at 37°C but not at 26°C promotes hDC-SIGN- and mSIGNR1-mediated invasion of host cells. hDC-SIGN is a receptor for *E. coli* and other Gram-negative bacteria with rough-type LPS (14, 26). Furthermore, we have unpublished evidence suggesting that the *Y. pestis* LOS uses the mouse SIGNR1, not the mouse DC-SIGN, SIGNR3, or langerin (mCD207), as a receptor. To investigate whether human DC-SIGN and mouse SIGNR1 were responsible for the interaction of human DCs and mouse macrophages, stably transfected cell lines expressing human DC-SIGN (HeLa-hDC-SIGN) and murine SIGNR1 (CHO-mSIGNR1) were tested for their

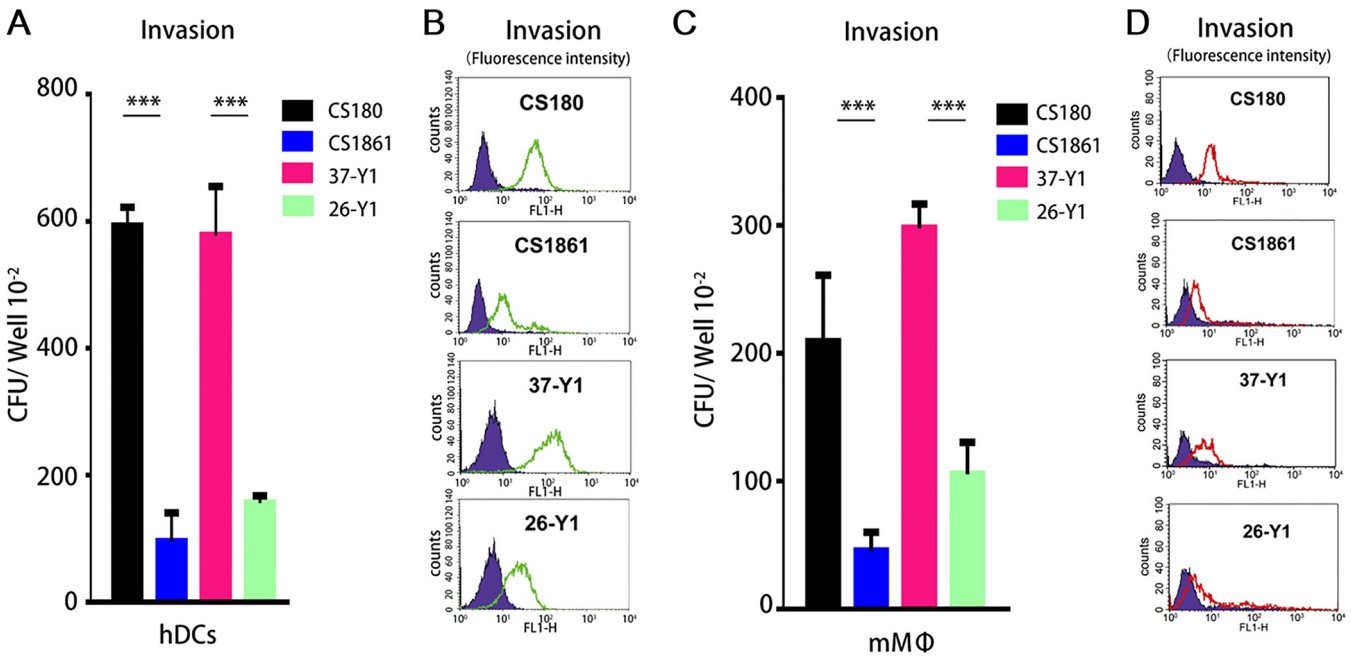

FIG 3 *Y. pseudotuberculosis* cultured at 37°C but not 26°C invades human DCs and murine macrophages. Gentamicin protection- and flow cytometry-based assays were used to determine the DC invasion rates of *Y. pseudotuberculosis* Y1. *E. coli* K-12 strains (CS180 and CS1861) were utilized as controls. (A and C) Data from the gentamicin protection assay. (B and D) Data from flow cytometry. DCs and macrophages incubated with labeled and unlabeled bacteria are indicated by open and filled curves, respectively. *Y. pseudotuberculosis* organisms cultured at 37°C and 26°C are referred to as 37-Y1 and 26-Y1, respectively. ***, $P < 0.001$.

ability to phagocytose Y1 bacteria grown at 37°C and 26°C (37-Y1 and 26-Y1, respectively). Again, *E. coli* CS180 and CS1861 bacteria were used as controls.

Two observations were made from these experiments (Fig. 4). First, 26-Y1 bacteria invaded all cells (HeLa, HeLa-hDC-SIGN, CHO, and CHO-mSIGN-R1) at similar rates, indicating that neither hDC-SIGN nor mSIGNR1 was necessary for the invasion. In *Y. pseudotuberculosis*, three invasion factors, invasin, YadA, and Ail, participate in the host-pathogen interactions (21, 23, 27). Very likely, the very effective hDC-SIGN/mSIGNR1-independent interaction with HeLa and CHO cells (Fig. 4A and B) is mediated by interaction between invasin and its receptor, β-integrin, which is expressed on most epithelial cells (20, 21). Second, 37-Y1 bacteria invaded HeLa-hDC-SIGN (Fig. 4A) and CHO-mSIGNR1 (Fig. 4B) cells more effectively than HeLa-Neo and CHO-Neo cells. It

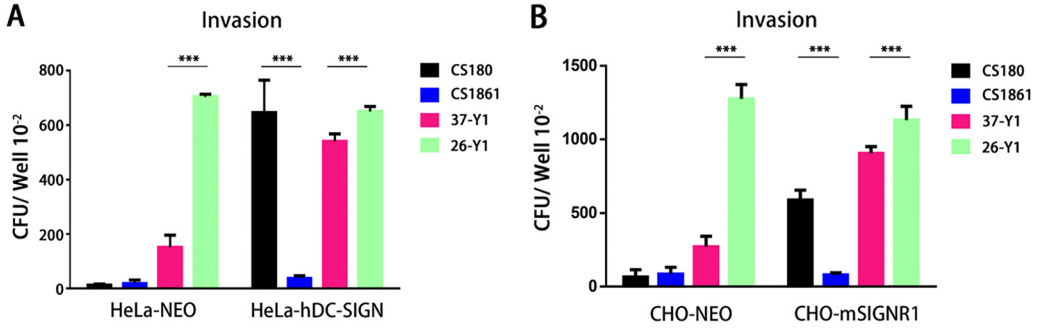

FIG 4 HeLa-hDC-SIGN and CHO-mSIGNR1 transfectants phagocytose *Y. pseudotuberculosis* grown at 37°C. The phagocytosis of two pairs of bacteria, *E. coli* K-12 (CS180 and CS1861) and *Y. pseudotuberculosis* Y1, cultured at 26°C and 37°C with HeLa/HeLa-hDC-SIGN (A) and CHO/CHO-mSIGNR1 (B), was performed by incubating cell lines for 2 h with indicated bacterial strains and by killing the extracellular bacteria with gentamicin as described in Materials and Methods. The number of phagocytosed bacteria was determined by counting CFU recovered following gentamicin treatment. ***, $P < 0.001$.

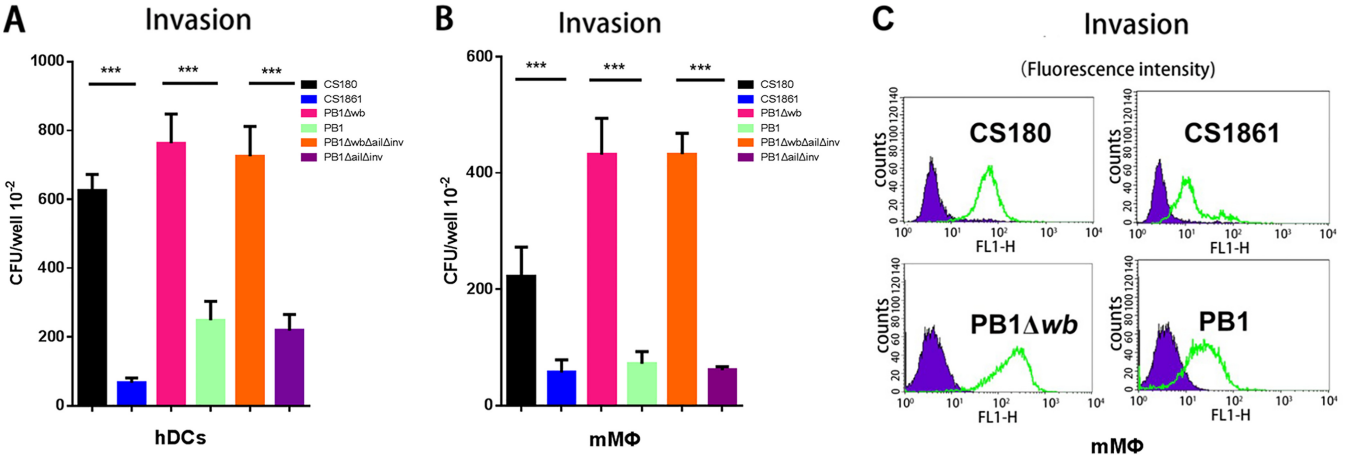

FIG 5 Human DCs and mouse macrophages phagocytose the defined rough *Y. pseudotuberculosis*. The phagocytosis of *Y. pseudotuberculosis* by human DCs (A) and mouse macrophages (B) followed the same procedures as those described in the legend to Fig. 3. The two strains used were the smooth LPS-producing *Y. pseudotuberculosis* PB1 and its isogenic rough derivative, the PB1Δ*wb* strain, lacking the O-ag. (A and B) Data from the gentamicin protection assay. (C) Data from flow cytometry. DCs and macrophages with labeled and unlabeled bacteria are indicated by open and filled curves, respectively. ***, $P < 0.001$.

should be noted that the invasion rate of 37-Y1 bacteria into HeLa cells was lower than that of 26-Y1 bacteria, as invasin expression is repressed at 37°C (28).

Based on the evidence described above, we conclude that hDC-SIGN and mSIGNR1 function as receptors and contribute to the phagocytosis of 37-Y1 in cell lines.

The LPS core of *Y. pseudotuberculosis* serves as a ligand. The data described above revealed similar invasion patterns of HeLa-hDC-SIGN and CHO-mSIGNR1 cells for *E. coli* CS180 and 37-Y1. Since the LPS core of *E. coli* is a ligand for hDC-SIGN (26), we speculated that the interaction of 37-Y1 bacteria with hDC-SIGN and mSIGNR1 would also be due to the exposed LPS core.

To confirm this hypothesis, we tested the interaction of two isogenic pairs of *Y. pseudotuberculosis* strains, PB1 and PB1Δ*wb* strains and PB1Δ*ailΔinv* and PB1Δ*wb*Δ*ail*Δ*inv* strains, with human DCs (Fig. 5A), mouse macrophages (Fig. 5B), HeLa or HeLa-hDC-SIGN cells, and CHO or CHO-mSIGN-R1 cells (Fig. 6A and B). It should be noted that the wild-type *Y. pseudotuberculosis* strain PB1 produces smooth LPS, and its PB1Δ*wb* rough isogenic derivative produces LOS (29, 30). In addition, for this experiment, the virulent plasmid in PB1 and its isogenic derivatives was deleted.

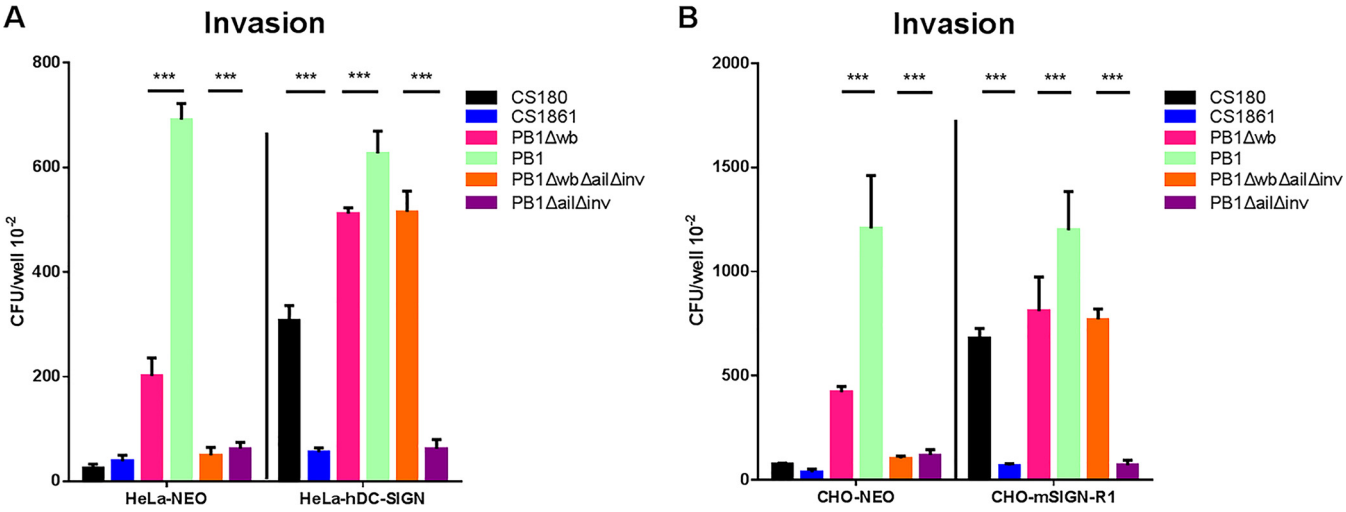

FIG 6 Human DC-SIGN and mouse SIGNR1 transfectants phagocytose the rough *Y. pseudotuberculosis*. The invasion of HeLa-hDC-SIGN (A) and CHO-mSIGNR1 (B) with PB1/PB1Δ*wb* and PB1Δ*ailΔinv*/PB1Δ*wb*Δ*ailΔinv* strains followed the same procedures as described for Fig. 4. ***, $P < 0.001$.

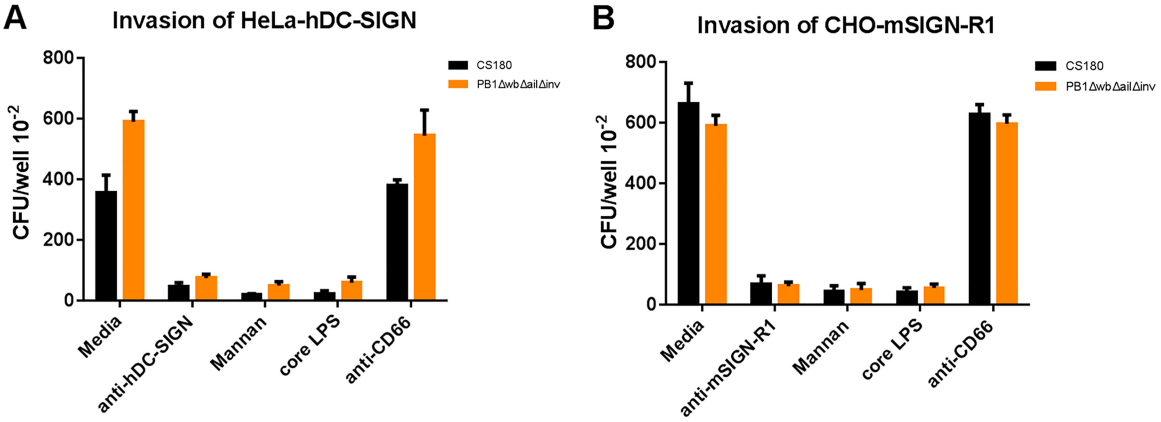

FIG 7 Phagocytosis of *Y. pseudotuberculosis* PB1Δ*wb*Δ*ail*Δ*inv* strain by HeLa-DC-SIGN and CHO-mSIGN-R1 was blocked by anti-hDC-SIGN antibody, anti-mSIGN-R1 antibody, mannan, and LPS core. (A) Pretreated HeLa-NEO and HeLa-hDC-SIGN cells with anti-hDC-SIGN antibody, mannan, and LPS core were incubated for 2.5 h with the *Y. pseudotuberculosis* PB1Δ*wb*Δ*ail*Δ*inv* strain. Bacterial phagocytosis was measured as described in Materials and Methods. (B) Pretreatment of cells with anti-mSIGN-R1 antibody, mannan, and LPS core blocked phagocytosis of the *Y. pseudotuberculosis* PB1Δ*wb*Δ*ail*Δ*inv* strain to CHO-mSIGN-R1. $P < 0.001$.

As shown in Fig. 6, the rough PB1Δ*wb* bacteria with or without an *inv*- and *ail*-deleting background, even when grown at 26°C, promoted the very typical core-mediated interaction with hDC-SIGN (26) and mSIGNR1, whereas the smooth PB1 did not. Taken together, the ability of rough *Y. pseudotuberculosis* to interact with human DCs, mouse macrophages, HeLa-hDC-SIGN, and CHO-mSIGN-R1 cells is most likely due to interactions between the exposed LPS core and hDC-SIGN and mSIGN-R1.

The interactions between LPS core and hDC-SIGN/mSIGN-R1 were inhibited by additions of anti-hDC-SIGN/mSIGN-R1, mannan, and LPS core oligosaccharides. To confirm that LPS core of *Y. pseudotuberculosis* is involved in the interaction, we examined whether the interactions of HeLa-hDC-SIGN and CHO-mSIGN-R1 transfectants with rough *Y. pseudotuberculosis* could be inhibited by anti-hDC-SIGN antibody, anti-mSIGN-R1 antibody, mannan, which specifically binds mannose-related receptors, and LPS core. Anti-CD66 antibody was used as a control antibody. As shown in Fig. 7A and B, the invasion of HeLa-hDC-SIGN and CHO-mSIGNR1 by the PB1Δ*wb*Δ*ail*Δ*inv* strain was blocked by addition of all three inhibitors.

Although the anti-hDC-SIGN, mannan, and LPS core failed to show any significant impact on the phagocytosis of *Y. pseudotuberculosis* of the PB1Δ*wb*Δ*ail*Δ*inv* strain, when used separately (Fig. 8), this hDC-rough *Y. pseudotuberculosis* interaction showed a reduction when the triple reagents were applied. In our previous studies, we found that anti-DC-SIGN antibody alone cannot effectively inhibit the LPS core-mediated phagocytosis of *E. coli*, *Neisseria gonorrhoeae,* and *Y. pestis* by DCs (14, 26, 31–33). We speculated that other receptors also are involved in the phagocytosis of the core-exposed Gram-negative bacteria. Details are addressed in Discussion.

The LPS core-mediated phagocytosis of *Y. pseudotuberculosis* by macrophages occurs *in vivo*. While it is clear that the LPS core participates in the *in vitro* interaction of *Y. pseudotuberculosis* with APCs, it remained to be elucidated whether this interaction also occurs *in vivo*. To this end, we injected bacterial suspensions directly into the intraperitoneal cavity of live mice. This approach is analogous to our previous study showing that the interaction of mouse CD205 (DEC-205) receptor on alveolar macrophages with the *Y. pestis* plasminogen activator (Pla) occurs *in vivo* (34). The intraperitoneal exudate was collected from the mice 1.5 h after the infection and placed in gentamicin medium to kill the extracellular bacteria. Figure 9 shows that a higher percentage of the PB1Δ*wb* bacteria than of the wild-type PB1 strains were intracellular and, thus, protected from gentamicin killing.

The data suggest that the LPS core interaction with mSIGNR1 had mediated phagocytosis of *Y. pseudotuberculosis* by macrophages *in vivo*.

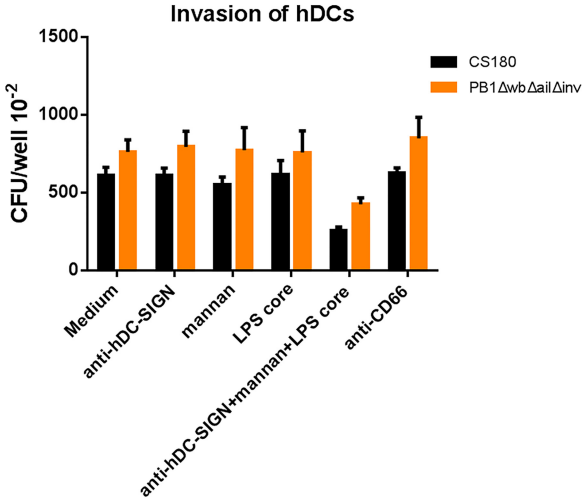

FIG 8 Reduction of phagocytosis of *Y. pseudotuberculosis* PB1Δ*wb*Δ*ail*Δ*inv* strain by DCs in the presence of anti-DC-SIGN, mannan, and LPS core together. Besides the addition of anti-hDC-SIGN, mannan, and LPS core, the procedures followed were the same as those described for DCs in the legend to Fig. 5A. $P < 0.001$ by two-way ANOVA comparing the interaction of DCs with *Y. pseudotuberculosis* PB1Δ*wb*Δ*ail*Δ*inv* strain in the presence of anti-hDC-SIGN, mannan, and LPS core to the interaction in the absence of antibody.

The exposure of the LPS core enhances the dissemination of *Y. pseudotuberculosis* to MLNs, spleen, and liver. We have demonstrated here that *Y. pseudotuberculosis*, when grown at 37°C, uses its LPS core to interact with hDC-SIGN and mSIGNR1 receptors, leading to the invasion of APCs *in vitro* and *in vivo*. We therefore hypothesized that the dissemination of *Y. pseudotuberculosis* to the MLNs, spleens, and livers would also be a result of this host-pathogen interaction. Subsequently, shielding the exposed LPS core of *Y. pseudotuberculosis* grown *in vivo* at 37°C should reduce the dissemination of the bacteria to MLNs, spleens, and livers.

(i) Higher numbers of rough than smooth *Y. pseudotuberculosis* bacteria were disseminated to MLNs, spleens, and livers. To achieve a *Y. pseudotuberculosis* strain producing smooth LPS *in vivo*, we introduced plasmid pAY100.1 into strain Y1. Plasmid pAY100.1 carries the O-ag gene cluster of *Y. enterocolitica* serotype O:3 and produces the O-ag irrespective of the growth temperature (31, 32, 34–36). As a control, the plasmid vector pBR322 was transformed to Y1. Mice were infected via the orogastric route with Y1/pBR322 and Y1/pAY100.1 bacteria and sacrificed after 72 h. MLNs, livers, and spleens were then recovered and homogenized. The dissemination rates of the

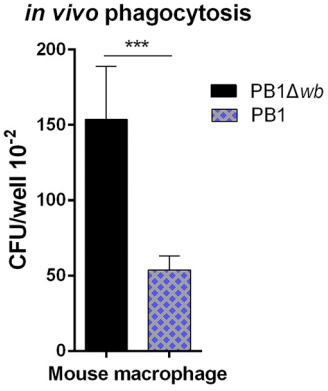

FIG 9 Interaction of the LPS core with macrophages occurs *in vivo*. Bacterial suspensions of PB1Δ*wb* and PB1 strains, cultured at 26°C, were inoculated into the intraperitoneal cavity of live mice. After incubation for 1.5 h, collected macrophages were examined for the rate of internalized bacteria. ***, $P < 0.001$.

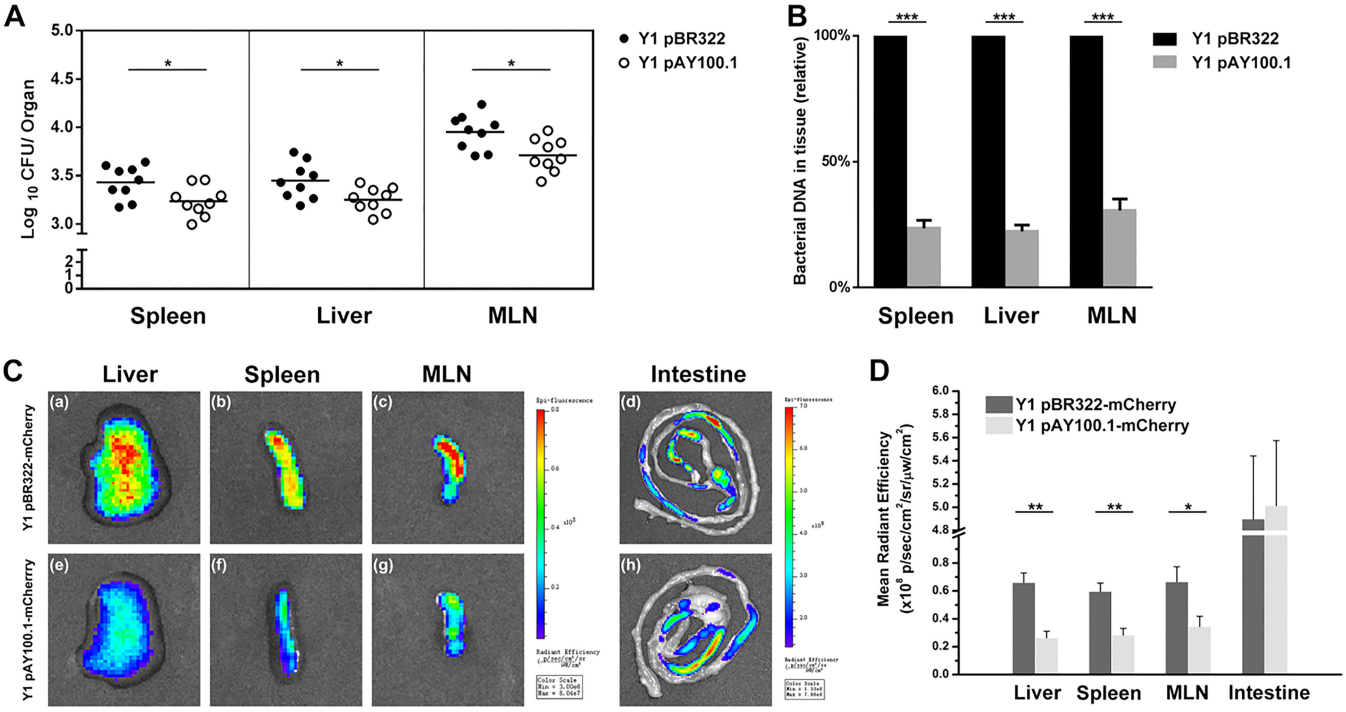

FIG 10 Dissemination of *Y. pseudotuberculosis* was inhibited when covered with O-ag. Mice were infected orogastrically with 10^8 CFU of Y1/pBR322 or Y1/pAY100.1, and bacterial loads in the spleens, livers, and MLNs were quantified at 72 h postinfection. (A) For CFU counting, the homogenized samples of organs were spread on LB agar to recover the bacteria. Each circle represents the data obtained for one infected mouse, and horizontal boldface lines indicate the median values. *, $P < 0.05$. (B) Eight hours after inoculation in the real-time PCR assay, the absolute numbers of bacteria were determined from standard curves of serial dilutions of Y1 chromosome DNA. Values obtained from three independent measurements represent Y1/pAY100.1 DNA extracted from total tissue relative to that of Y1/pBR322. ***, $P < 0.001$. (C) After infection with Y1/pBR322-mCherry or Y1/pAY100.1-mCherry, mice were sacrificed and the spleens, livers, MLNs, and intestine were isolated for detection with the IVIS system, as shown in panel D. **, $P < 0.005$.

bacteria into the different organs were calculated by counting CFU. Figure 10A and C shows that higher numbers of Y1/pBR322 than Y1/pAY100.1 bacteria were isolated from the MLNs, spleens, and livers. Importantly, no differences in bacterial numbers were observed between the intestinal lumens of Y1/pBR322- and Y1/pAY100.1-infected mice (Fig. 10D). In addition, both strains exhibited no differences in growth and adhered to both HeLa and CHO cells equally well (data not shown).

(ii) Higher quantity of bacterial DNA was recovered from MLNs, livers, and spleens of mice infected with rough than with smooth *Y. pseudotuberculosis*. The mice were challenged as described above, but the mice were sacrificed after 8 h of infection. The *Y. pseudotuberculosis*-specific DNA in MLNs, livers, and spleens was quantitated using *ail* gene-specific real-time PCR. In all tissues the relative amount of bacterial DNA was higher in Y1/pBR322- than in Y1/pAY100.1-infected mice (Fig. 10B), supporting the results of bacterial numbers described above.

In summary, the results suggest that *Y. pseudotuberculosis* could utilize its LPS core to interact with CD209 to enhance dissemination to the host tissues.

Blocking of the LPS core CD209 interaction with mannan or dextran oligosaccharide reduces the infectivity of *Y. pseudotuberculosis*. The LPS core CD209 interaction in *E. coli* can be blocked *in vitro* by several oligosaccharides, including mannan (14). Given that the interactions reported above were mediated by the LPS core oligosaccharide, we hypothesized that shielding the exposed LPS core with CD209-interacting oligosaccharides could reduce the bacterial infectivity in a murine model. To this end, we tested the influence of mannan and dextran oligosaccharides on the infectivity of the wild-type and fully virulent *Y. pseudotuberculosis* strain YPIII (37). The body weights and the mortality of the mice were monitored. The results clearly demonstrated that both the body weight loss (Fig. 11A) and mortality rate (Fig. 11B) of mice infected with YPIII in the presence of mannan or dextran oligosaccharides were

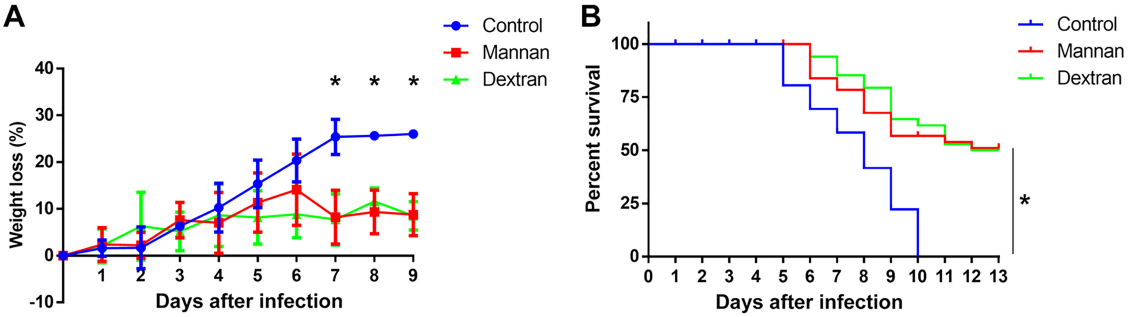

FIG 11 Blockage of the host-pathogen interaction with certain oligosaccharides reduces the infectivity by *Y. pseudotuberculosis*. After culture at 37°C, wild-type *Y. pseudotuberculosis* strain YPIII (37) bacteria with or without mannan or dextran were inoculated into mice by following procedures described in Materials and Methods. The rates of body weight loss (A) and mortality (B) were recorded every 12 h up to 156 h postinfection. Student's *t* test was used to determine significant differences in both body weight and death of mice by the wild-type *Y. pseudotuberculosis* YPIII with and without oligosaccharides, mannan, and dextran. *, $P < 0.001$.

significantly reduced. It should be noted that the growth rate of the *Y. pseudotuberculosis* YPIII bacteria was not influenced by the mannan oligosaccharide, as is the case with other Gram-negative bacteria (14, 26, 33).

In conclusion, these results might help us understand how and why oligosaccharide-based prevention methods and treatments for certain diarrheal infections work.

DISCUSSION

Y. pseudotuberculosis is able to disseminate and infect MLNs (10). However, the molecular mechanisms involved in dissemination of *Y. pseudotuberculosis* to MLNs remained to be determined. In this work, we demonstrate that the interaction between LPS core oligosaccharide and CD209 receptors may contribute to this dissemination.

O-ag is a well-documented virulence factor for *Y. pseudotuberculosis*, but O-ag production was almost fully suppressed in bacteria grown at 37°C (17–19), suggesting that during infection the LPS core oligosaccharide of the bacteria was exposed (Fig. 1). Why would *Y. pseudotuberculosis* restrain the expression of its virulence factor during infection? Based on the evidence presented in this work, we speculate that after penetration through the mucosal membrane of the small intestine, perhaps not via Peyer's patches (Fig. 2), *Y. pseudotuberculosis* intentionally represses O-ag production. This exposes the LPS core oligosaccharide to interact with CD209. As a result, the bacteria invade the APCs and are carried by the infected APCs to lymph nodes, spleen, and liver, facilitating the bacteria to colonize these tissues and establish the host infection.

Thus, an important corollary to this study is that some pathogens, such as *Y. pseudotuberculosis*, have evolved mechanisms for exploiting the very host defenses designed to eliminate them, with the result being an expanded ability to disseminate. Our unpublished data also indicate that similar to *Y. pseudotuberculosis*, *Salmonella*, but not *Shigella*, is able to modify its LPS during infection. Consequently, *Salmonella* is also able to hijack the APCs in a manner similar to that of *Y. pseudotuberculosis*.

Certain technical issues need to be discussed here. First, three identified virulence factors mediate interactions between *Y. pseudotuberculosis* bacteria and host cells (21, 23, 27), one of which is invasin. As shown in Fig. 4, *Y. pseudotuberculosis* cultured at 26°C interacts with HeLa and CHO cells at a high level, but this interaction was reduced when *Y. pseudotuberculosis* was cultured at 37°C, since the expression of invasin at this temperature is suppressed (28). On the other hand, it appears that invasin does not participate in or influence the interaction between *Y. pseudotuberculosis* and dendritic cells, because *Y. pseudotuberculosis* cultured at 37°C invades DCs, but the invasion of DC by *Y. pseudotuberculosis* cultured at 26°C is dramatically reduced.

Besides the integrin-invasin interaction, *Y. pseudotuberculosis* promotes another hDC-SIGN- or mSIGNR1-independent interaction with HeLa and CHO cells (Fig. 4 and 6). We have observed that this DC-SIGN-independent interaction appears to rely on the Ail protein of *Yersinia,* which may involve the heparan sulfate proteoglycan (our unpub-

lished observation) and other binding proteins of fibronectin (38), C4b-binding protein (39), and vitronectin (40). Fortunately, this interaction can be inhibited by heparin, a synthetic form of heparan sulfate (31). This is also the reason for the inclusion of heparin in the experiments intended to observe the interaction between *Y. pseudotuberculosis* and HeLa or CHO cells (Fig. 4 and 6).

We showed that a clear inhibition was obtained from transfectants (Fig. 7) but not in primary cells (Fig. 8). Only the triple reagents of inhibitors (antireceptor antibodies, mannan oligosaccharide, and purified LPS core) employed were able to partially inhibit the interactions of hDCs with *Y. pseudotuberculosis*. There might be many reasons or factors involving the interaction in primary cells. (i) As described above, we believe the interaction between LPS core carbohydrates and C-type lectins results from nonspecific bindings, i.e., while some cell lines are capable of these interactions, primary cells are not. (ii) Human DCs also expressed langerin (CD207), another receptor for HIV, which was also a receptor for the LPS core (32). (iii) DCs are very dynamic cells that phagocytose everything they encounter.

We have suggested that suppression of O-ag expression in *Y. pseudotuberculosis* enhances its virulence, but the fact is that the expression of O-ag is absolutely necessary for the pathogenicity based on the recovery of a number of O-ag gene cluster mutants in signature-tagged mutagenesis experiments (41). Therefore, we used the *Y. pseudotuberculosis* strain Y1, grown at 26°C and at 37°C, instead of the PB1 and PB1Δ*wb* strains to examine the LPS core CD209 interaction-mediated *in vivo* dissemination (Fig. 10). For this reason, this study only indicates that in *Y. pseudotuberculosis* the O-ag expression is repressed during certain stages of the infection and/or in different tissues.

DC-SIGN (CD209), langerin (CD207), and DEC-205 (CD205) have been shown to be receptors for the LPS core ligand of several Gram-negative bacterial species, thereby promoting bacterial adherence and phagocytosis (14, 26, 31–34). The biological significance of the host-pathogen interaction has been poorly understood and ill-defined. The present study provides the first instance of a definition of this interaction and its possible biological significance, which may contribute to future studies in various fields, as shown below.

Salmonella spp. rather than *Shigella* spp. are able to disseminate to other parts of mammalian organs and cause systemic infections. Ongoing studies in the laboratory indicate that like *Y. pseudotuberculosis*, *Salmonella* spp., but not *Shigella* spp., are able to modify their full O-antigen-expressing LPS into O-antigen deletion core LOS during infection. Consequently, *Salmonella* spp. (data not shown) are able to hijack the APCs similarly to the infection caused by *Y. pseudotuberculosis*, as described in this study. As shown in our previous report, *S. enterica* serovar Typhimurium utilizes its core LOS to interact with human DC-SIGN, resulting in phagocytosis by host cells (14). Interestingly, a recent report indicated that *Shigella* spp. are able to disseminate if the expression of O-antigen or O-antigen-expressing capsule is genetically modified (42). It should be recognized that the previous report categorized results for *Shigella* and *E. coli* as being from a single species.

The most significant contribution of this study is to reveal a possibly new molecular mechanism of several persistent infections, including urinary tract infection (UTI) by *E. coli*, Gram-negative bacterium-associated Crohn's disease, typhoid fever, *Helicobacter pylori*-associated chronic atrophic gastritis (ChAG), and chronic infection caused by *Klebsiella* spp. Although the expression of O-antigen protects the Gram-negative bacterial pathogens from phagocytosis and serum killing, the core LOS-expressing bacteria (rough strains), such as enterohemorrhagic *E. coli* (EHEC), uropathogenic *E. coli* (UPEC), *Salmonella* spp., *Helicobacter pylori*, *Shigella sonnei*, and *Y. pseudotuberculosis*, are isolated from clinical samples (14, 26). We expect that the loss of O-antigen or modification of LPS during infection causes the Gram-negative bacteria to become less virulent but readily phagocytosed by APCs. Thus, the phagocytosed bacteria may hide themselves from attacks of various host clearance systems, as shown in *Salmonella* (43). Mounting data have shown associations among APCs, C-type lectin CD209s, LPS, and

persistent infections caused by the Gram-negative bacterial pathogens described above. Hopefully, the data presented in this work will add to the collective understanding.

Y. pseudotuberculosis is an ancestor of several Gram-negative bacteria (7–9, 44, 45), can live and replicate in various host niches (46), and causes different clinical manifestations (47). Studies of this pathogen during infection may generate a broad impact in understanding the pathogenesis of bacterial pathogens in general. A new technology, called dual RNA sequencing (RNA-seq), for monitoring the transcript profiles of pathogens and hosts during infection has been developed (48). This technology has been used for profiling *S. enterica* serovar Typhimurium (49), *Haemophilus influenzae* (50), and *Mycobacterium tuberculosis* (51); these profiles were limited to *in vitro* studies only. With *Y. pseudotuberculosis* as the model strain, Nuss et al. further established a fast, generic tissue dual RNA-seq approach, which allows a broad and instantaneous monitoring of gene expression that links the infected hosts and the colonizing pathogens in *in vivo* infection (52). As a result, they first found that one of the main strategies for bacterial survival during infection was to prevent pathogens from phagocytic attacks (52). Second, they discovered that *Yersinia* germs can also reduce the production of toxins that induce the inflammation of the afflicted tissues during infection. Therefore, the reduction of inflammation allows bacteria to escape attacks from the host immune system (53). This process is now named "bacteria persist as stowaways" (https://health.economictimes.indiatimes.com/news/industry/bacteria-persist-as-stowaways-hzi/62836896). The toxin described here could be the O-antigen of *Y. pseudotuberculosis*.

In summary, because this host-pathogen interaction is not restricted to one species, the findings presented here may contribute to future, more broad studies, as also illustrated in the last sentence of a 2006 report (14): "From an evolutionary point of view, the interaction of bacterial core LOS/LPS and the innate immune receptor, DC-SIGN, may represent a primitive interaction between microbial pathogens and the professional phagocytic host cells."

MATERIALS AND METHODS

Human and animal studies. All animal procedures and human experiments were carried out in strict accordance with the Institutional Animal Care and Use Committees (IACUCs) and Institutional Review Board (IRB) of Tongji Hospital, Tongji Medical College, Tongji, China. The handling of the mice and all experimental procedures were specifically approved for this study by the Medical Ethics Committee of Tongji Hospital and were conducted in accordance with institutional guidelines (IRB identifiers TJ-A20141220 for animal experiments and TJC20140113 for human experiments). All procedures on mice were performed under sodium pentobarbital anesthesia, all efforts were made to minimize suffering, and all volunteers involved in the experiment signed informed consent.

Bacterial strains. *E. coli* K-12 strain CS180 produces a rough LPS missing O-ag (54) (Table 1). CS1861 is a derivative of CS180 harboring pSS37, a plasmid containing all of the genes for O-ag expression from *Shigella dysenteriae* 1 (54–56) (Fig. 1). *E. coli* strains were cultured on Luria-Bertani (LB) medium supplemented with 1.5% agar at 37°C overnight. *Y. pseudotuberculosis* Y1 is a serotype O:1a strain lacking the virulence plasmid (pYV). This strain originates from the CDC and has been used as a positive invasion control previously (57–59). We also used the *Y. pseudotuberculosis* O:1a wild-type strain PB1 (60) and its rough isogenic derivative, the PB1Δ*wb* strain, which is unable to produce O-ag due to deletion of the whole O-ag gene cluster (29). Constructions of *inv*- and *ail*-deleting mutants for PB1 are also shown in Table 1. These strains were grown and maintained in a manner identical to that for *E. coli* K-12. The *Yersinia* strains described above were virulence plasmid-cured strains, selected using a combination of magnesium oxalate and Congo red selection methods (61). However, *Yersinia pseudotuberculosis* serotype O:3 strain YPIII is a wild-type and fully virulent strain (37) and contains the virulence plasmid.

Construction of *Y. pseudotuberculosis* that expresses O-ag at 37°C. The lack of O-ag at 37°C in *Y. pseudotuberculosis* is due to repression of the O-ag biosynthetic genes (17–19) (Fig. 1). *Y. pseudotuberculosis* strain Y1 was transformed with plasmid pAY100.1, which carries all of the necessary genes for the expression of the O-ag of *Y. enterocolitica* serotype O:3 (35, 36). The expression of O-antigen, coded for by pAY100.1 plasmid, is not influenced by growth temperature (31, 32, 34). Therefore, this mutant is still able to express a full LPS even at 37°C.

Construction of *Y. pseudotuberculosis* PB1 and PB1Δ*wb* strains with *inv* and *ail* gene knockout. We used two steps to construct the *inv*- and *ail*-deleted mutants. First, to knock out the *ail* gene of *Y. pseudotuberculosis*, the suicide plasmid PCVD442-ail::KmGB was mobilized into the *Y. pseudotuberculosis* PB1Δ*wb* strain, as described previously by Ho et al. (62) and our laboratory (unpublished data). Briefly, the suicide plasmid in *E. coli* S17-1λpir was introduced into the parental *Y. pseudotuberculosis* PB1Δ*wb* strain by conjugation. The Kan^r transconjugants were selected using a *Yersinia* selective agar plate with cefsulodin-irgasan-novobiocin (CIN) agar for counterselection of the donor. The selected transconjugants

TABLE 1 Bacterial strains and cell lines used in this study

Strain or cell line	Genotype (phenotype) or characteristic	Reference or source
Y. pseudotuberculosis strains		
Y1	Serotype O:1a, wild type expressing invasin, but with pYV plasmid naturally cured	74
PB1	Serotype O:1a, wild type	60
PB1Δ*ail*	*ail*::Kan^r, Km^r, derivative of PB1	62
PB1Δ*ail*Δ*inv*	PB1Δ*ail* with the *inv* gene knockout	This study
PB1Δ*wb*	Serotype O:1a, O-PS-negative derivative of PB1, Kan^r	29
PB1Δ*wb*Δ*ail*Δ*inv*	PB1Δ*wb* strain with the *ail* and *inv* gene double KO	This study
Y1/pBR322	Y1 with pBR322 plasmid; O-ag expression suppressed at 37°C	This study
Y1/pAY100.1	Y1 with pAY100.1 plasmid expressing *Y. enterocolitica* O:3 O-ag	This study
Y1/pBR322-mCherry	Y1/pBR322 with mCherry plasmid	This study
Y1/pAY100.1-mCherry	Y1/pAY100.1 with mCherry plasmid	This study
YPIII	Serotype O:3	37
E. coli K-12 strains		
CS180	Wild type	54–56
CS1861	CS180-O antigen	
S17-1 λpir	*thi pro* Δ*hsdR hsdM*$^+$ *recA*::RP4-2-Tc::μ-Km::Tn*7 strR* (λ*pir*)	62
Cell lines		
HeLa-NEO	Control cell line, which expresses the neomycin resistance gene only	
HeLa-DC-SIGN	Generated by transfecting HeLa cells with human DC-SIGN cDNAs for stable surface expression	
CHO-NEO	Control cell line, which expresses the neomycin resistance gene only	
CHO-SIGNR1	Generated by transfecting CHO cells with mouse SIGNR1 cDNAs for stable surface expression	

then were plated onto LB agar with 10% sucrose and grown at room temperature for 2 days. The correct allelic exchange in the resultant Suc^r Kan^r colonies was confirmed using PCR with corresponding primers ailrf1 (5-TCAATGGGGCTATTGATTTCG-3) and ailr1 (5-GGTGACTTGCTCGAAATAATG-3) (63). Replacement of Ail with a cassette results in a complete deletion of the *ail* gene. The deletion of the *ail* gene from the mutants resulted in the PB1Δ*wb*Δ*ail* strain.

For generating the *inv* knockout strain, the CRISPR-Cas12a system was used to delete the *inv* gene from the *Y. pseudotuberculosis* PB1Δ*ail* and PB1Δ*wb*Δ*ail* strains, as described previously (64, 65). Briefly, the protospacer adjacent motif (PAM) TTG, a short DNA sequence (3 to 5 bp) adjacent to the protospacer (target, 25 nucleotides [nt]) site, was selected in the coding sequence of *inv*. Two complementary oligonucleotides (crRNA-inv top and crRNA-inv bottom) containing the protospacer sequence (adjacent to 5′-TTG-3′) were synthesized, annealed to yield a protospacer cassette with BsaI overhangs at the 5′ and 3′ ends, and then cloned into the crRNA expression plasmid pAC-crRNA-Cm to generate the recombinant plasmid pcrRNA-inv-Cm. A single-stranded DNA (ssDNA) oligonucleotide (*inv* oligonucleotide for lagging) with 40 nt of flanking region sequence identity on both sides of the mutation site was synthesized, in which 3 termination codons (TAA TGA TAG) and a 22-nt random sequence were introduced between the 2 flanking regions. Cotransformation of the ssDNA oligonucleotides and the recombinant plasmid pcrRNA-inv-Cm into *Y. pseudotuberculosis PB1*Δ*ail* and *PB1*Δ*wb*Δ*ail* cells harboring pKD46-cpf1(Cas12a) was performed, and samples were plated on LB supplemented with 100 μg/ml ampicillin and 30 μg/ml chloramphenicol and incubated at 26°C. Single colonies were plucked to inoculate LB medium supplemented with appropriate antibiotics at 26°C. We performed PCR on the target gene regions with corresponding primers to screen preliminarily and sent the PCR products for sequencing to verify the PB1Δ*ail*Δ*inv* and PB1Δ*wb*Δ*ail*Δ*inv* clones. Finally, the pcrRNA-inv-Cm plasmid and pKD46-cpf1 plasmid were cured by incubation on an LB plate with 7% sucrose and incubation in LB medium at 42°C with shaking overnight, respectively.

Biochemical and cellular biology reagents. Mannan oligosaccharide (M-7504) and dextran oligosaccharide (CAS; 9004-54-0) were purchased from Sigma-Aldrich (St. Louis, MO) and Aladdin (Shanghai, China), respectively. Anti-human DC-SIGN and mouse SIGNR1 monoclonal antibodies (MAbs) were purchased from Pharmingen (San Diego, CA). LPS core of *Neisseria gonorrhoeae* was purified as described previously (66). The bacteria were suspended in water and heated to 65°C. Equal volumes of phenol heated to 65°C were added to the bacterial suspensions, and the mixture was incubated at 65°C for 1 h with stirring. After centrifugation, the aqueous phase was recovered and the interfacial/phenol phase material was reextracted once with water. Aqueous phases were ultrafiltered three times through a 100-kDa ultrafiltration device (Millipore), ultracentrifuged at 100,000 × *g* for 6 h, and lyophilized.

Mice. C57BL/6, BALB/cJ, and LTβR-1 KO mice in the C57BL/6 background (25) were bred in the animal facility of UIC–College of Medicine and Tongji Hospital or purchased from Wuhan University Animal Center. Mice were housed in animal facilities at the UIC–College of Medicine and Tongji Hospital in direct accordance with guidelines drafted by the Animal Care Committees of UIC–College of Medicine–Rockford and Tongji Hospital. The peritoneal macrophages express high levels of SIGNR1 (67, 68), as shown in Fig. 9B.

Preparation of DCs. Peripheral blood mononuclear cells (PBMC) were isolated from buffy coats obtained from human blood donors by density gradient centrifugation over FicollPaque^{plus} (1.077 g/ml; Pharmacia, Piscataway, NJ). Blood was loaded in a 1:1 (vol/vol) ratio on Ficoll and centrifuged without

braking for 30 min. PBMC were washed 4 times with phosphate-buffered saline (PBS), and monocytes were purified from PBMC using CD14 microbeads (Miltenyi Biotec, Auburn, CA), as previously described (69). To increase purity, cells were passed over a second CD14 microbead column. The final purity of the isolated monocytes was >98%, as assessed by labeling with CD14-fluorescein isothiocyanate (FITC) antibody (Caltag, Carlsbad, CA) and flow cytometric analysis. Purified $CD14^+$ monocytes (5×10^5 cells/ml) were cultured for 6 days to promote differentiation of immature monocyte-derived DCs (MDDCs) in culture medium consisting of RPMI 1640 (BioWhittaker, Walkersville, MD), 10% heat-inactivated fetal bovine serum (FBS) (HyClone, Logan, UT), 100 U/ml penicillin, and 100 μg/ml streptomycin in the presence of 20 ng/ml recombinant human granulocyte macrophage colony-stimulating factor (Immunex, Seattle, WA) and 10 ng/ml recombinant human interleukin-4 (Peprotech, Rock Hill, NJ). The DCs derived from these cultured monocytes display typical dendrites, and in mixed lymphocyte cultures they promote activation of alloreactive T cells. The phenotypes of these cells are $HLA\text{-}DR^+$, $CD1a^+$, $CD86^+$, $CD40^+$, and $CD14^-$ (69). Upon LPS stimulation, these DCs express CD83 (70). We have utilized this protocol for identification of DC-SIGN as a receptor for core LPS of several Gram-negative bacteria and to explore how *N. gonorrhoeae* enhances HIV infection (14, 26, 31, 66).

Isolation of mouse peritoneal macrophages. After the mice were euthanized, the abdomens of mice were immediately exposed, cleaned with 70% ethanol, and opened with scissors. Five milliliters of RPMI was injected into the intraperitoneal cavity. Mouse abdomen was gently massaged for 2 min, and then the lavage fluid was collected. The suspension containing the macrophages was seeded onto 6-well plates, in which each well contained a 1.5-cm-diameter glass coverslide, and placed in a CO_2 incubator for 2 h. The cell layers were washed 3 times to remove nonadherent cells. Macrophages were then removed from the plastic surface by incubation with citrate saline and reseeded for interaction assays.

Cell lines. HeLa-hDC-SIGN cells were generated by transfecting HeLa cells with human DC-SIGN cDNA, followed by selection for stable surface DC-SIGN expression, as originally described (71) (Table 1). The cell lines were recently used for identification of core LPS from several Gram-negative bacteria as the ligand for the DC-SIGN receptor (14, 26, 33).

Mouse C-type lectin transfectant, CHO-mSIGNR1, was generated by transfecting CHO cells with mouse SIGNR1 cDNAs, followed by selection for stable surface expression as originally described (67). CHO-NEO is a control cell line which expresses the neomycin resistance gene only.

Adherence and phagocytosis assays. The adherence and phagocytosis assays were carried out as described previously (59, 72). Briefly, host cells (HeLa, CHO, dendritic cells, and human and mouse macrophages) were plated in 24- or 96-well plates. Cells were suspended in RPMI with 2% fetal calf serum (FCS) at a concentration of 4×10^5/ml. Aliquots (0.5 ml each) of these cell suspensions of were added to 24-well plates, and after addition of 50 μl of bacterial suspensions at a concentration of 1×10^7 CFU/ml, the cells were allowed to incubate for 2.5 h (2 h for dendritic cells and alveolar macrophages) at 37°C in the presence of 5% CO_2. The cell monolayers were then washed 3 times with PBS. The number of associated bacteria (adherent and internalized) per cell was quantified by washing the cells 3 times with RPMI containing 2% FCS and plating the culture after the cells were lysed by 0.5% saponin (Calbiochem Corp., San Diego, CA).

To determine the internalization of bacteria, gentamicin, which kills extracellular bacteria but cannot penetrate into host cells, was added into each well to a final concentration of 100 μg/ml, and the cultures were incubated for 60 min. Cells were washed twice to remove the antibiotic (for DCs, a cytospin was necessary during the washing, since DCs do not attach to plastic wells). Cells were suspended in PBS containing 0.5% saponin, diluted, and plated on GC or LB plates. The level of internalization of bacteria in these host cells was calculated by determining the CFU recovered from lysed cells. All experiments were performed in triplicate, and data are expressed as means ± standard errors.

Determination of phagocytosis by flow cytometry. The following method was used to supplement the survival-based phagocytosis assay described above, since DCs kill some phagocytosed bacteria, such as *Neisseria gonorrhoeae* (14, 33, 34). Measurement of the phagocytosis rate of bacteria by DCs was performed as follows. Briefly, bacteria were suspended in RPMI medium containing 5- and 6-carboxyfluorescein diacetate-succinimidyl ester (CFDA-SE; Molecular Probes, Eugene, OR) for 40 min and washed 2 times with RPMI to remove the excess dye. Labeled bacteria were added to DC cultures for 2 h. Cell cultures were washed 2 times to remove unbound bacteria. DCs plus associated bacteria were fixed with 2% paraformaldehyde. Before flow cytometry, a 1:10 dilution of Trypan blue (0.4%, Sigma, St. Louis, MO) was added to the fixed cell cultures, and the mixture was incubated at ambient temperature for 10 min (33) to quench the fluorescence from extracellular labeled bacteria. Trypan blue blocks fluorescence but cannot penetrate host cells; therefore, fluorescence from internalized bacteria will not be influenced by addition of Trypan blue. The rate of bacterial internalization was determined by comparing the percentage of fluorescence-positive DCs with that of DCs interacting with unlabeled bacteria.

***In vivo* phagocytosis assays for peritoneal macrophages.** The protocol for the *in vivo* phagocytosis assay is derived from a similar procedure from our previous studies on alveolar macrophages (34). In detail, 1 ml of bacterial suspension (optical density at 600 nm [OD_{600}] of 0.1) was injected into the mouse intraperitoneal cavity. Mouse abdomen was gently massaged for 1 min. After 1.5 h, mice were euthanized, another 4 ml of RPMI with 2% FCS was immediately injected into each mouse intraperitoneal cavity, and the abdomen was gently massaged for another 1 min. The intraperitoneal fluids or exudates were collected, and the numbers of cells were counted for each collection of intraperitoneal lavage. A total of 1×10^6 cells were seeded onto each well of 24-well plates, containing RPMI with 2% FCS and gentamicin at a concentration of 100 μg/ml, and were then incubated for 1.5 h to allow the macrophages to adhere to plates and kill the extracellular bacteria. Each well was washed three times with RPMI with

2% FCS to remove nonadhered cells and lysed with saponin by following the same procedures as those for the *in vitro* phagocytosis assays described above.

Animal challenging for dissemination and infection. C57BL/6, BALB/cJ, and LTβR-1 KO mice in the C57BL/6 background (25) were used in the following experiments. The dissemination rate was defined as the transport of *Y. pseudotuberculosis* to MLNs, livers, and spleens of the mice. The infectivity was defined as the body weight loss and the mortality after inoculations of pathogens.

In detail, mice were inoculated with *Y. pseudotuberculosis* at an OD_{600} of 1.0 in phosphate-buffered saline (0.3 ml) via the orogastric route with a catheter. In experiments with strains Y1/pBR322 and Y1/pAY100.1, mice were injected intravenously with 50 μg/g ampicillin on each of the following days. At 72 h postinoculation, mice were euthanized and MLNs, livers, and spleens were collected and homogenized. It should be noted that MLNs isolated here included whole mesentery tissues. (i) For CFU determination, the homogenized organs were lysed with 1% Triton X-100 to release the bacteria 10 min before they were plated onto LB agar containing ampicillin. The numbers of CFU per organ were determined as described previously (34). (ii) For real-time PCR assay, after 8 h of inoculation, total DNA was isolated from the tissue-homogenized samples recovered from mice infected with *Y. pseudotuberculosis*. A standard dilution series of purified genomic *Y. pseudotuberculosis* DNA at concentrations of 10^8, 10^7, 10^6, 10^5, 10^4, 10^3, 10^2, 10, and 1 copies/μl was used for quantification. The standard dilution series was included in all PCR runs. Primers amplified a 157-bp fragment from the *ail* gene and were the following: forward, CGTCTGTTAATGTGTATGCCGAAG; reverse, GAACCTATCACTCCCCAGTCATTATT. The real-time PCR was performed with a SYBR Green master mix and detected with a LightCycler (73). The threshold cycle of each sample was measured for two replicates, and the DNA concentrations were calculated using the LightCycler software. (iii) For *in vivo* imaging, Y1/pBR322-mCherry and Y1/pAY100.1-mCherry, derived from Y1/pBR322 and Y1/pAY100.1, respectively, were used. The IVIS Spectrum *in vivo* imaging system detected the mCherry fluorescent protein with filters covering its excitation and emission wavelengths at 587 nm and 610 nm. To better define the infected areas, the individual organs, instead of whole mouse body, were collected and detected under the imaging system. Two points should be noted. First, 30 min before inoculation, mice were injected with ampicillin at a final concentration of 50 μg/g of mouse body weight to maintain the plasmid-based expression of O-antigen in Y1/pAY100.1. Second, the *Y. pseudotuberculosis* strains used in this study were cultured at 26°C in order to get effective invasion of mucosal surfaces. As mentioned in Discussion, the expression of invasin is inhibited at 37°C (28). (iv) For the animal challenge assay, after growth at 37°C, wild-type *Y. pseudotuberculosis* YPIII, pretreated with and without oligosaccharides, was inoculated at an OD_{600} of 0.2 in a manner similar to that described for the *in vivo* dissemination assay. The rates of body weight and death of the mice were recorded every 12 h up to 156 h postinfection.

Statistical analyses. All statistical analyses were completed using Prism software, version 6 (Graph Pad, San Diego, CA, USA). Statistical significance was assessed using Student's *t* test for the univariate analysis of two sets of data and two-way analysis of variance (ANOVA) for multiple comparisons; for mouse survival experiments (Fig. 11B), we used the log-rank test.

SUPPLEMENTAL MATERIAL

Supplemental material for this article may be found at https://doi.org/10.1128/IAI.00654-18.

SUPPLEMENTAL FILE 1, PDF file, 0.1 MB.

ACKNOWLEDGMENTS

This work was supported by a PHS grant (R01AI 47736 to T.C.) for work performed at the University of Illinois at Chicago and by grants from the National Natural Science Foundation of China (NSFC 81271780 and 81471915) and two local grants from Tongji Hospital, Tongji Medical College, to T.C. C.G.P. was supported by grants from the National Research Foundation of Korea (NRF-2013R1A1A2058427 and NRF-2014R1A4A1008625) and a faculty research grant of the Yonsei University College of Medicine for 2014 (6-2014-0062).

We thank Olivier Schwartz at Pasture Institute, Paris, and Joseph Hinnebusch at the Rocky Mountain Laboratories, NIH, for their long-term support and help to initiate the project regarding DC-SIGN and *Yersinia* species interactions. We are indebted to Ralph Steinman when he was at the Rockefeller University for his insightful advice and generous financial support for this project. Finally, we thank the Tongji Hospital, HUST, for their support and allowing this project to continue. We do not have a commercial or other association that poses a conflict of interest.

REFERENCES

1. Savin C, Martin L, Bouchier C, Filali S, Chenau J, Zhou Z, Becher F, Fukushima H, Thomson NR, Scholz HC, Carniel E. 2014. The *Yersinia pseudotuberculosis* complex: characterization and delineation of a new species, *Yersinia wautersii*. Int J Med Microbiol 304:452–463. https://doi.org/10.1016/j.ijmm.2014.02.002.
2. Bos KI, Schuenemann VJ, Golding GB, Burbano HA, Waglechner N,

Coombes BK, McPhee JB, DeWitte SN, Meyer M, Schmedes S, Wood J, Earn DJ, Herring DA, Bauer P, Poinar HN, Krause J. 2011. A draft genome of *Yersinia pestis* from victims of the Black Death. Nature 478:506–510. https://doi.org/10.1038/nature10549.

3. Haensch S, Bianucci R, Signoli M, Rajerison M, Schultz M, Kacki S, Vermunt M, Weston DA, Hurst D, Achtman M, Carniel E, Bramanti B. 2010. Distinct clones of *Yersinia pestis* caused the black death. PLoS Pathog 6:e1001134. https://doi.org/10.1371/journal.ppat.1001134.
4. Harbeck M, Seifert L, Hansch S, Wagner DM, Birdsell D, Parise KL, Wiechmann I, Grupe G, Thomas A, Keim P, Zoller L, Bramanti B, Riehm JM, Scholz HC. 2013. *Yersinia pestis* DNA from skeletal remains from the 6(th) century AD reveals insights into Justinianic Plague. PLoS Pathog 9:e1003349. https://doi.org/10.1371/journal.ppat.1003349.
5. Wagner DM, Klunk J, Harbeck M, Devault A, Waglechner N, Sahl JW, Enk J, Birdsell DN, Kuch M, Lumibao C, Poinar D, Pearson T, Fourment M, Golding B, Riehm JM, Earn DJ, Dewitte S, Rouillard JM, Grupe G, Wiechmann I, Bliska JB, Keim PS, Scholz HC, Holmes EC, Poinar H. 2014. *Yersinia pestis* and the plague of Justinian 541-543 AD: a genomic analysis. Lancet Infect Dis 14:319–326. https://doi.org/10.1016/S1473-3099(13)70323-2.
6. Bullock GL, Stuckey HM, Shotts EB, Jr. 1978. Enteric redmouth bacterium: comparison of isolates from different geographic areas. J Fish Dis 1:351–356. https://doi.org/10.1111/j.1365-2761.1978.tb00039.x.
7. Achtman M, Morelli G, Zhu P, Wirth T, Diehl I, Kusecek B, Vogler AJ, Wagner DM, Allender CJ, Easterday WR, Chenal-Francisque V, Worsham P, Thomson NR, Parkhill J, Lindler LE, Carniel E, Keim P. 2004. Microevolution and history of the plague bacillus, *Yersinia pestis*. Proc Natl Acad Sci U S A 101:17837–17842. https://doi.org/10.1073/pnas.0408026101.
8. Achtman M, Zurth K, Morelli G, Torrea G, Guiyoule A, Carniel E. 1999. *Yersinia pestis*, the cause of plague, is a recently emerged clone of *Yersinia pseudotuberculosis*. Proc Natl Acad Sci U S A 96:14043–14048. https://doi.org/10.1073/pnas.96.24.14043.
9. Morelli G, Song Y, Mazzoni CJ, Eppinger M, Roumagnac P, Wagner DM, Feldkamp M, Kusecek B, Vogler AJ, Li Y, Cui Y, Thomson NR, Jombart T, Leblois R, Lichtner P, Rahalison L, Petersen JM, Balloux F, Keim P, Wirth T, Ravel J, Yang R, Carniel E, Achtman M. 2010. *Yersinia pestis* genome sequencing identifies patterns of global phylogenetic diversity. Nat Genet 42:1140–1143. https://doi.org/10.1038/ng.705.
10. Weber J, Finlayson NB, Mark JB. 1970. Mesenteric lymphadenitis and terminal ileitis due to *yersinia pseudotuberculosis*. N Engl J Med 283:172–174. https://doi.org/10.1056/NEJM197007232830404.
11. Barnes PD, Bergman MA, Mecsas J, Isberg RR. 2006. *Yersinia pseudotuberculosis* disseminates directly from a replicating bacterial pool in the intestine. J Exp Med 203:1591–1601. https://doi.org/10.1084/jem.20060905.
12. Watson KG, Holden DW. 2010. Dynamics of growth and dissemination of *Salmonella* in vivo. Cell Microbiol 12:1389–1397. https://doi.org/10.1111/j.1462-5822.2010.01511.x.
13. Vazquez-Torres A, Jones-Carson J, Baumler AJ, Falkow S, Valdivia R, Brown W, Le M, Berggren R, Parks WT, Fang FC. 1999. Extraintestinal dissemination of *Salmonella* by CD18-expressing phagocytes. Nature 401:804–808. https://doi.org/10.1038/44593.
14. Zhang P, Snyder S, Feng P, Azadi P, Zhang S, Bulgheresi S, Sanderson KE, He J, Klena J, Chen T. 2006. Role of N-acetylglucosamine within core lipopolysaccharide of several species of Gram-negative bacteria in targeting the DC-SIGN (CD209). J Immunol 177:4002–4011. https://doi.org/10.4049/jimmunol.177.6.4002.
15. Geijtenbeek TB, Kwon DS, Torensma R, van Vliet SJ, van Duijnhoven GC, Middel J, Cornelissen IL, Nottet HS, KewalRamani VN, Littman DR, Figdor CG, van Kooyk Y. 2000. DC-SIGN, a dendritic cell-specific HIV-1-binding protein that enhances trans-infection of T cells. Cell 100:587–597. https://doi.org/10.1016/S0092-8674(00)80694-7.
16. McDonald D, Wu L, Bohks SM, KewalRamani VN, Unutmaz D, Hope TJ. 2003. Recruitment of HIV and its receptors to dendritic cell-T cell junctions. Science 300:1295–1297. https://doi.org/10.1126/science.1084238.
17. Bengoechea JA, Brandenburg K, Seydel U, Diaz R, Moriyon I. 1998. *Yersinia pseudotuberculosis* and *Yersinia pestis* show increased outer membrane permeability to hydrophobic agents which correlates with lipopolysaccharide acyl-chain fluidity. Microbiology 144(Part 6):1517–1526. https://doi.org/10.1099/00221287-144-6-1517.
18. Skurnik M. 2003. Molecular genetics, biochemistry and biological role of *Yersinia* lipopolysaccharide. Adv Exp Med Biol 529:187–197. https://doi.org/10.1007/0-306-48416-1_38.
19. Skurnik M, Bengoechea JA. 2003. The biosynthesis and biological role of lipopolysaccharide O-antigens of pathogenic *Yersiniae*. Carbohydr Res 338:2521–2529. https://doi.org/10.1016/S0008-6215(03)00305-7.
20. Isberg RR, Leong JM. 1988. Cultured mammalian cells attach to the invasin protein of *Yersinia pseudotuberculosis*. Proc Natl Acad Sci U S A 85:6682–6686. https://doi.org/10.1073/pnas.85.18.6682.
21. Isberg RR, Voorhis DL, Falkow S. 1987. Identification of invasin: a protein that allows enteric bacteria to penetrate cultured mammalian cells. Cell 50:769–778. https://doi.org/10.1016/0092-8674(87)90335-7.
22. Miller VL, Bliska JB, Falkow S. 1990. Nucleotide sequence of the *Yersinia enterocolitica* ail gene and characterization of the Ail protein product. J Bacteriol 172:1062–1069. https://doi.org/10.1128/jb.172.2.1062-1069.1990.
23. Miller VL, Falkow S. 1988. Evidence for two genetic loci in *Yersinia enterocolitica* that can promote invasion of epithelial cells. Infect Immun 56:1242–1248.
24. Miller VL, Farmer JJ, III, Hill WE, Falkow S. 1989. The ail locus is found uniquely in Yersinia enterocolitica serotypes commonly associated with disease. Infect Immun 57:121–131.
25. Wang Y, Koroleva EP, Kruglov AA, Kuprash DV, Nedospasov SA, Fu YX, Tumanov AV. 2010. Lymphotoxin beta receptor signaling in intestinal epithelial cells orchestrates innate immune responses against mucosal bacterial infection. Immunity 32:403–413. https://doi.org/10.1016/j.immuni.2010.02.011.
26. Klena J, Zhang P, Schwartz O, Hull S, Chen T. 2005. The core lipopolysaccharide of *Escherichia coli* is a ligand for the dendritic-cell-specific intercellular adhesion molecule nonintegrin CD209 receptor. J Bacteriol 187:1710–1715. https://doi.org/10.1128/JB.187.5.1710-1715.2005.
27. Bliska JB, Copass MC, Falkow S. 1993. The *Yersinia pseudotuberculosis* adhesin YadA mediates intimate bacterial attachment to and entry into HEp-2 cells. Infect Immun 61:3914–3921.
28. Pepe JC, Badger JL, Miller VL. 1994. Growth phase and low pH affect the thermal regulation of the *Yersinia enterocolitica inv* gene. Mol Microbiol 11:123–135. https://doi.org/10.1111/j.1365-2958.1994.tb00295.x.
29. Kiljunen S, Datta N, Dentovskaya SV, Anisimov AP, Knirel YA, Bengoechea JA, Holst O, Skurnik M. 2011. Identification of the lipopolysaccharide core of *Yersinia pestis* and *Yersinia pseudotuberculosis* as the receptor for bacteriophage phiA1122. J Bacteriol 193:4963–4972. https://doi.org/10.1128/JB.00339-11.
30. Kukkonen M, Suomalainen M, Kyllonen P, Lahteenmaki K, Lang H, Virkola R, Helander IM, Holst O, Korhonen TK. 2004. Lack of O-antigen is essential for plasminogen activation by *Yersinia pestis* and *Salmonella enterica*. Mol Microbiol 51:215–225. https://doi.org/10.1046/j.1365-2958.2003.03817.x.
31. Zhang P, Skurnik M, Zhang SS, Schwartz O, Kalyanasundaram R, Bulgheresi S, He JJ, Klena JD, Hinnebusch BJ, Chen T. 2008. Human dendritic cell-specific intercellular adhesion molecule-grabbing nonintegrin (CD209) is a receptor for *Yersinia pestis* that promotes phagocytosis by dendritic cells. Infect Immun 76:2070–2079. https://doi.org/10.1128/IAI.01246-07.
32. Yang K, Park CG, Cheong C, Bulgheresi S, Zhang S, Zhang P, He Y, Jiang L, Huang H, Ding H, Wu Y, Wang S, Zhang L, Li A, Xia L, Bartra SS, Plano GV, Skurnik M, Klena JD, Chen T. 2015. Host Langerin (CD207) is a receptor for *Yersinia pestis* phagocytosis and promotes dissemination. Immunol Cell Biol 93:815–824. https://doi.org/10.1038/icb.2015.46.
33. Zhang P, Schwartz O, Pantelic M, Li G, Knazze Q, Nobile C, Radovich M, He J, Hong SC, Klena J, Chen T. 2006. DC-SIGN (CD209) recognition of *Neisseria gonorrhoeae* is circumvented by lipooligosaccharide variation. J Leukoc Biol 79:731–738. https://doi.org/10.1189/jlb.0405184.
34. Zhang SS, Park CG, Zhang P, Bartra SS, Plano GV, Klena JD, Skurnik M, Hinnebusch BJ, Chen T. 2008. Plasminogen activator Pla of *Yersinia pestis* utilizes murine DEC-205 (CD205) as a receptor to promote dissemination. J Biol Chem 283:31511–31521. https://doi.org/10.1074/jbc.M804646200.
35. Al-Hendy A, Toivanen P, Skurnik M. 1991. Expression cloning of *Yersinia enterocolitica* O:3 rfb gene cluster in *Escherichia coli* K12. Microb Pathog 10:47–59. https://doi.org/10.1016/0882-4010(91)90065-I.
36. Oyston PC, Prior JL, Kiljunen S, Skurnik M, Hill J, Titball RW. 2003. Expression of heterologous O-antigen in *Yersinia pestis* KIM does not affect virulence by the intravenous route. J Med Microbiol 52:289–294. https://doi.org/10.1099/jmm.0.05044-0.
37. Bolin I, Norlander L, Wolf-Watz H. 1982. Temperature-inducible outer membrane protein of *Yersinia pseudotuberculosis* and *Yersinia enterocolitica* is associated with the virulence plasmid. Infect Immun 37:506–512.
38. Tsang TM, Annis DS, Kronshage M, Fenno JT, Usselman LD, Mosher DF,

Krukonis ES. 2012. Ail protein binds ninth type III fibronectin repeat (9FNIII) within central 120-kDa region of fibronectin to facilitate cell binding by *Yersinia pestis*. J Biol Chem 287:16759–16767. https://doi.org/10.1074/jbc.M112.358978.
39. Ho DK, Skurnik M, Blom AM, Meri S. 2014. *Yersinia pestis* Ail recruitment of C4b-binding protein leads to factor I-mediated inactivation of covalently and noncovalently bound C4b. Eur J Immunol 44:742–751. https://doi.org/10.1002/eji.201343552.
40. Bartra SS, Ding Y, Miya Fujimoto L, Ring JG, Jain V, Ram S, Marassi FM, Plano GV. 2015. *Yersinia pestis* uses the Ail outer membrane protein to recruit vitronectin. Microbiology 161:2174–2183. https://doi.org/10.1099/mic.0.000179.
41. Karlyshev AV, Oyston PC, Williams K, Clark GC, Titball RW, Winzeler EA, Wren BW. 2001. Application of high-density array-based signature-tagged mutagenesis to discover novel *Yersinia* virulence-associated genes. Infect Immun 69:7810–7819. https://doi.org/10.1128/IAI.69.12.7810-7819.2001.
42. Caboni M, Pedron T, Rossi O, Goulding D, Pickard D, Citiulo F, MacLennan CA, Dougan G, Thomson NR, Saul A, Sansonetti PJ, Gerke C. 2015. An O antigen capsule modulates bacterial pathogenesis in *Shigella sonnei*. PLoS Pathog 11:e1004749. https://doi.org/10.1371/journal.ppat.1004749.
43. Helaine S, Cheverton AM, Watson KG, Faure LM, Matthews SA, Holden DW. 2014. Internalization of *Salmonella* by macrophages induces formation of nonreplicating persisters. Science 343:204–208. https://doi.org/10.1126/science.1244705.
44. Cui Y, Yu C, Yan Y, Li D, Li Y, Jombart T, Weinert LA, Wang Z, Guo Z, Xu L, Zhang Y, Zheng H, Qin N, Xiao X, Wu M, Wang X, Zhou D, Qi Z, Du Z, Wu H, Yang X, Cao H, Wang H, Wang J, Yao S, Rakin A, Li Y, Falush D, Balloux F, Achtman M, Song Y, Wang J, Yang R. 2013. Historical variations in mutation rate in an epidemic pathogen, *Yersinia pestis*. Proc Natl Acad Sci U S A 110:577–582. https://doi.org/10.1073/pnas.1205750110.
45. Spyrou MA, Tukhbatova RI, Feldman M, Drath J, Kacki S, Beltran de Heredia J, Arnold S, Sitdikov AG, Castex D, Wahl J, Gazimzyanov IR, Nurgaliev DK, Herbig A, Bos KI, Krause J. 2016. Historical *Y. pestis* genomes reveal the European Black Death as the source of ancient and modern plague pandemics. Cell Host Microbe 19:874–881. https://doi.org/10.1016/j.chom.2016.05.012.
46. Moreau K, Lacas-Gervais S, Fujita N, Sebbane F, Yoshimori T, Simonet M, Lafont F. 2010. Autophagosomes can support *Yersinia pseudotuberculosis* replication in macrophages. Cell Microbiol 12:1108–1123. https://doi.org/10.1111/j.1462-5822.2010.01456.x.
47. Gossman WG, Bhimji SS. 2018. Yersinia pseudotuberculosis. StatPearls, Treasure Island, FL.
48. Westermann AJ, Gorski SA, Vogel J. 2012. Dual RNA-seq of pathogen and host. Nat Rev Microbiol 10:618–630. https://doi.org/10.1038/nrmicro2852.
49. Westermann AJ, Forstner KU, Amman F, Barquist L, Chao Y, Schulte LN, Muller L, Reinhardt R, Stadler PF, Vogel J. 2016. Dual RNA-seq unveils noncoding RNA functions in host-pathogen interactions. Nature 529:496–501. https://doi.org/10.1038/nature16547.
50. Baddal B, Muzzi A, Censini S, Calogero RA, Torricelli G, Guidotti S, Taddei AR, Covacci A, Pizza M, Rappuoli R, Soriani M, Pezzicoli A. 2015. Dual RNA-seq of nontypeable Haemophilus influenzae and host cell transcriptomes reveals novel insights into host-pathogen cross talk. mBio 6:e01765-15. https://doi.org/10.1128/mBio.01765-15.
51. Rienksma RA, Suarez-Diez M, Mollenkopf HJ, Dolganov GM, Dorhoi A, Schoolnik GK, Martins Dos Santos VA, Kaufmann SH, Schaap PJ, Gengenbacher M. 2015. Comprehensive insights into transcriptional adaptation of intracellular mycobacteria by microbe-enriched dual RNA sequencing. BMC Genomics 16:34. https://doi.org/10.1186/s12864-014-1197-2.
52. Nuss AM, Beckstette M, Pimenova M, Schmuhl C, Opitz W, Pisano F, Heroven AK, Dersch P. 2017. Tissue dual RNA-seq allows fast discovery of infection-specific functions and riboregulators shaping host-pathogen transcriptomes. Proc Natl Acad Sci U S A 114:E791–E800. https://doi.org/10.1073/pnas.1613405114.
53. Heine W, Beckstette M, Heroven AK, Thiemann S, Heise U, Nuss AM, Pisano F, Strowig T, Dersch P. 2018. Loss of CNFY toxin-induced inflammation drives *Yersinia pseudotuberculosis* into persistency. PLoS Pathog 14:e1006858. https://doi.org/10.1371/journal.ppat.1006858.
54. Schnaitman CA, Klena JD. 1993. Genetics of lipopolysaccharide biosynthesis in enteric bacteria. Microbiol Rev 57:655–682.
55. Klena JD, Ashford RS, II, Schnaitman CA. 1992. Role of *Escherichia coli* K-12 *rfa* genes and the *rfp* gene of *Shigella dysenteriae* 1 in generation of lipopolysaccharide core heterogeneity and attachment of O antigen. J Bacteriol 174:7297–7307. https://doi.org/10.1128/jb.174.22.7297-7307.1992.
56. Klena JD, Schnaitman CA. 1993. Function of the *rfb* gene cluster and the *rfe* gene in the synthesis of O antigen by *Shigella dysenteriae* 1. Mol Microbiol 9:393–402. https://doi.org/10.1111/j.1365-2958.1993.tb01700.x.
57. Chen T, Belland RJ, Wilson J, Swanson J. 1995. Adherence of pilus- Opa+ gonococci to epithelial cells in vitro involves heparan sulfate. J Exp Med 182:511–517. https://doi.org/10.1084/jem.182.2.511.
58. Chen T, Gotschlich EC. 1996. CGM1a antigen of neutrophils, a receptor of gonococcal opacity proteins. Proc Natl Acad Sci U S A 93:14851–14856. https://doi.org/10.1073/pnas.93.25.14851.
59. Chen T, Grunert F, Medina-Marino A, Gotschlich E. 1997. Several carcinoembryonic antigens (CD66) serve as receptors for gonococcal opacity proteins. J Exp Med 185:1557–1564. https://doi.org/10.1084/jem.185.9.1557.
60. Porat R, McCabe WR, Brubaker RR. 1995. Lipopolysaccharide-associated resistance to killing of *Yersiniae* by complement. J Endotoxin Res 2:91–97. https://doi.org/10.1177/096805199500200203.
61. Riley G, Toma S. 1989. Detection of pathogenic *Yersinia enterocolitica* by using Congo red-magnesium oxalate agar medium. J Clin Microbiol 27:213–214.
62. Ho DK, Riva R, Kirjavainen V, Jarva H, Ginstrom E, Blom AM, Skurnik M, Meri S. 2012. Functional recruitment of the human complement inhibitor C4BP to *Yersinia pseudotuberculosis* outer membrane protein Ail. J Immunol 188:4450–4459. https://doi.org/10.4049/jimmunol.1103149.
63. Felek S, Krukonis ES. 2009. The *Yersinia pestis* Ail protein mediates binding and Yop delivery to host cells required for plague virulence. Infect Immun 77:825–836. https://doi.org/10.1128/IAI.00913-08.
64. Li SY, Cheng QX, Wang JM, Li XY, Zhang ZL, Gao S, Cao RB, Zhao GP, Wang J. 2018. CRISPR-Cas12a-assisted nucleic acid detection. Cell Discov 4:20. https://doi.org/10.1038/s41421-018-0028-z.
65. Yan MY, Yan HQ, Ren GX, Zhao JP, Guo XP, Sun YC. 2017. CRISPR-Cas12a-assisted recombineering in bacteria. Appl Environ Microbiol 83:e00947-17. https://doi.org/10.1128/AEM.00947-17.
66. Zhang J, Li G, Bafica A, Pantelic M, Zhang P, Broxmeyer H, Liu Y, Wetzler L, He JJ, Chen T. 2005. *Neisseria gonorrhoeae* enhances the infection of dendritic cells by human immunodeficiency virus type-1 (HIV-1). J Immunol 174:7995–8002. https://doi.org/10.4049/jimmunol.174.12.7995.
67. Kang YS, Yamazaki S, Iyoda T, Pack M, Bruening SA, Kim JY, Takahara K, Inaba K, Steinman RM, Park CG. 2003. SIGN-R1, a novel C-type lectin expressed by marginal zone macrophages in spleen, mediates uptake of the polysaccharide dextran. Int Immunol 15:177–186. https://doi.org/10.1093/intimm/dxg019.
68. Takahara K, Yashima Y, Omatsu Y, Yoshida H, Kimura Y, Kang YS, Steinman RM, Park CG, Inaba K. 2004. Functional comparison of the mouse DC-SIGN, SIGNR1, SIGNR3 and Langerin, C-type lectins. Int Immunol 16:819–829. https://doi.org/10.1093/intimm/dxh084.
69. Li G, Kim YJ, Mantel C, Broxmeyer HE. 2003. P-selectin enhances generation of CD14+CD16+ dendritic-like cells and inhibits macrophage maturation from human peripheral blood monocytes. J Immunol 171:669–677. https://doi.org/10.4049/jimmunol.171.2.669.
70. Zhou LJ, Tedder TF. 1995. Human blood dendritic cells selectively express CD83, a member of the immunoglobulin superfamily. J Immunol 154:3821–3835.
71. Sol-Foulon N, Moris A, Nobile C, Boccaccio C, Engering A, Abastado J-P, Heard J-M, van Kooyk Y, Schwartz O. 2002. HIV-1 Nef-induced upregulation of DC-SIGN in dendritic cells promotes lymphocyte clustering and viral spread. Immunity 16:145–155. https://doi.org/10.1016/S1074-7613(02)00260-1.
72. Chen T, Bolland S, Chen I, Parker J, Pantelic M, Grunert F, Zimmermann W. 2001. The CGM1a (CEACAM3/CD66d) mediated phagocytic pathway of *Neisseria gonorrhoeae* expressing opacity (Opa) proteins is also the pathway to cell death. J Biol Chem 276:17413–17419. https://doi.org/10.1074/jbc.M010609200.
73. Cornelis G, Laroche Y, Balligand G, Sory MP, Wauters G. 1987. *Yersinia enterocolitica*, a primary model for bacterial invasiveness. Rev Infect Dis 9:64–87. https://doi.org/10.1093/clinids/9.1.64.
74. Samuelsson K, Lindberg B, Brubaker RR. 1974. Structure of O-specific side chains of lipopolysaccharides from *Yersinia pseudotuberculosis*. J Bacteriol 117:1010–1016.